CrossMark

Synthesis, characterization and controlled release properties of zinc–aluminium-beta-naphthoxyacetate nanocomposite

Zaemah binti Jubri[1] [ORCID] **· Nor Zalina Anua binti Mohd Yusoff[1] · Siti Halimah binti Sarijo[2] · Elya Sufliza binti Marsom[1] · Mohd Zobir bin Hussein[3]**

Abstract An organic–inorganic nanohybrid nanocomposite was synthesized by co-precipitation method using beta-naphthoxyacetate (BNOA) as guest anion and zinc–aluminium layered double hydroxide (Zn–Al-LDH) as the inorganic host. A well-ordered nanohybrid nanocomposite was formed when the concentration of BNOA was 0.08 M and the molar ratio of Zn to Al, R = 2. Basal spacing of layered double hydroxide containing nitrate ions expanded from 8.9 to 19.5 Å in resulting of Zn–Al-BNOA nanocomposite was obtained indicates that beta-naphthoxyacetate was successfully intercalated into interlayer spaces of layered double hydroxide. It was also found out the BET surface area increased from 1.13 to 42.79 $m^2\,g^{-1}$ for Zn–Al-LDH and Zn–Al-BNOA nanocomposite, respectively. The BJH average pore diameter of the synthesized nanocomposite is 199 Å which shows mesoporous-type of material. CHNS analysis shows the Zn–Al-BNOA nanocomposite material contains 36.2 % (w/w) of BNOA calculated based on the percentage of carbon in the sample. Release of BNOA from the lamella of Zn–Al-BNOA was controlled by the zeroth and first order kinetics at the beginning of the deintercalation process up to 200 min and controlled by pseudo-second order kinetics for the whole process. This study suggests that layered double hydroxide can be used as a carrier for organic acid herbicide controlled release formulation of BNOA.

Keywords Layered double hydroxide · Beta-naphthoxyacetate · Hydrotalcite · Herbicide · Nanocomposite

1 Introduction

The hydrotalcite like compounds, also called layered double hydroxide (LDH), have been investigated for many years. LDHs have been studied extensively for a wide range of applications utilizing catalysts [1], ion exchange [2], adsorbents [3], bio-organic nanohybrids [4], and also in pharmaceutical industry [5]. LDHs are a class of anionic clays with general formula $\left[M_{1-x}^{2+}M_x^{3+}(OH)_2\right]^{x+}\left[(X^{n-})_{x/n}\cdot H_2O\right]^{x-}$ where M^{2+} and M^{3+} are divalent and trivalent metal cations respectively, x is the ratio of $M^{3+}/(M^{2+} + M^{3+})$. The structure of an LDH is basically built up from the parent structure brucite, $Mg(OH)_2$ by isomorphous substitution of divalent cations [6]. The replacement of M^{2+} by M^{3+} ions generates an excess of positive charge within the inorganic layers, which has to be balanced by incorporation in the interlayer space of anions, X^{n-} such as NO_3^-, Cl^-, CO_3^{2-} and SO_4^{2-}. In addition to anions, the interlayer space region can also contain water molecules connected to the inorganic layers via hydrogen bonding [7].

Layered organic–inorganic nanohybrid materials can be prepared by propping apart the layered host and inserting guest molecules into the interlamellae of layered double hydroxide. A variety of anionic species could be intercalated for the formation of LDH-intercalated or so-called the host–

✉ Zaemah binti Jubri
zaemah@uniten.edu.my

[1] College of Engineering, Universiti Tenaga Nasional, 43009 Kajang, Selangor, Malaysia

[2] Faculty of Applied Science, Universiti Teknologi Mara, 40450 Shah Alam, Selangor, Malaysia

[3] Materials Synthesis and Characterization Laboratory, Institute of Advanced Technology, Universiti Putra Malaysia, 43400 Serdang, Selangor, Malaysia

guest type materials. The guest species enhance the interlayer distance in LDH compound and the thickness of the layer is determined by the ionic radius of anion. An intercalation reaction will leave the structure of the host lattice unchanged and therefore different from the normal solid state reactions that involve extensive bond breaking and structural reorganization [8].

Recently, there has been rapid expansion of the development of organic–inorganic nanohybrid system for various useful agents such as herbicides for controlled release formulations. This system can allow safe and controlled delivery of various useful agents into target with high efficiency. The controlled release formulations have several distinct advantages. They can minimize herbicides residue to the environment, maintain toxic concentrations of herbicide in close proximity to the target organism and increase the efficacy and longevity of the herbicide by protecting it from environmental degradation. Most traditional controlled release formulations are polymer-based but alternative inorganic matrices, particularly layered double hydroxides (LDHs) have attracted considerable recent attention [9].

In this paper, we report on the intercalation of the anions of beta-naphthoxyacetic acid (BNOA) into Zn–Al-LDH to form a new organic–inorganic nanohybrid material. The molecular structure of the BNOA ($C_{12}H_{10}O_3$) is shown in Fig. 1. It is a type of herbicides, which is used as a synthetic auxin similar to natural auxin such as indolebutyric acid (IBA) [10].

2 Materials and methods

2.1 Materials

Zinc nitrate hexahydrate [$Zn(NO_3)_2 \cdot 6H_2O$, Merck], aluminium nitrate nonahydrate, [$Al(NO_3)_3 \cdot 9H_2O$, Merck], sodium hydroxide [NaOH, Merck] and 2-naphthoxyacetic acid [$C_{12}H_{10}O_3$, Fluka] were purchased without further purification. Deionized water was degassed under nitrogen atmosphere to prevent carbon dioxide entering the solution and to avoid the formation of carbonic acid in the solutions.

2.2 Preparation of Zn–Al-BNOA nanocomposite

The synthesis of Zn–Al-BNOA nanocomposite was carried out by co-precipitation method. A solution containing $Zn(NO_3)_2$ and $Al(NO_3)_2$ with molar ratio of Zn/Al of 2 and BNOA at various concentration ranging from 0.06 to 0.10 M was mixed together. The pH of the solution was adjusted to pH 7.0 ± 0.2 by slow dropwise addition of 2.0 M NaOH. The reaction was carried out under nitrogen atmosphere. The solution was aged for 18 h in an oil bath shaker at 70 °C. The resulting precipitate was centrifuged, washed thoroughly with distilled water and dried in an oven at 70 °C. The sample was then kept in sample bottle for further use and characterization. A similar method was adopted for preparation of Zn–Al-LDH with nitrate as the intergallery anion except the addition of BNOA.

2.3 Characterization

Powder X-ray diffraction (PXRD) patterns were recorded by Shimadzu Diffractometer XRD-6000, using CuK$_\alpha$ ($\lambda = 1.54$ Å) at 40 kV and a scan range between 2° and 60°. Fourier transform infrared spectra (FTIR) were recorded using a Perkin-Elmer $1725\times$ in the range of 400–4000 cm^{-1}. A CHNS analyzer, model EA 1108 of Finons Instruments, was used to determine the percentage of carbon in Zn–Al-BNOA material. The elemental composition of Zn/Al molar ratio of the samples were determined by an inductively couple plasma emission spectrometry (ICP-AES) with a Perkin Elmer Spectrophotometer model optima 2000DV under standard condition. Determination of the surface area of the samples was carried out using Micromeritics surface area and porosity analyzer (ASAP 2000) using nitrogen gas adsorption–desorption technique at 77 K. Samples were degassed in an evacuated-heated chamber at 120 °C,

Fig. 1 The intercalation of beta-naphthoxyacetic acid (BNOA) into Zn–Al-LDH to form Zn–Al-BNOA

Zn-Al-LDH

BNOA

Zn-Al-BNOA
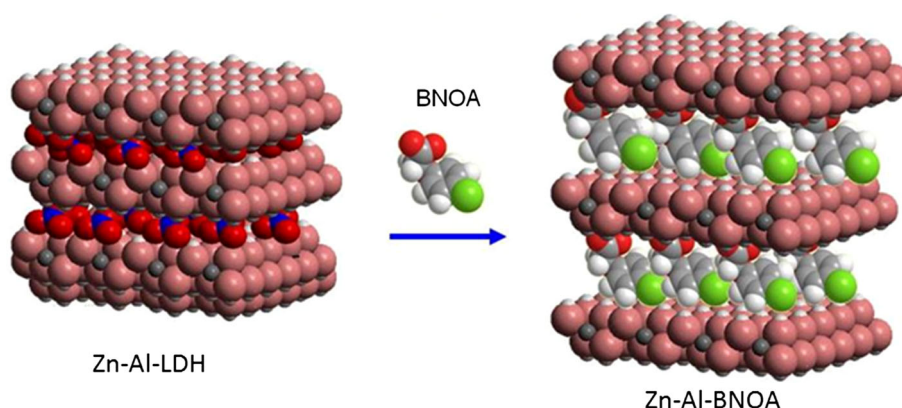
overnight prior the measurement. The surface morphology of the samples was observed by a field emission scanning electron microscope (FESEM), using Carl Zeiss Supra 40VP model.

2.4 Controlled release study of BNOA

The release of BNOA into aqueous solution was done using 0.17 mg of BNOA in 3.5 ml 0.005 M aqueous solutions of Na_3PO_4, Na_2CO_3, Na_2SO_4 and NaCl. The amount of BNOA released into the solution was measured insitu at $\lambda_{max} = 271.1$ nm using a Perkin Elmer UV–Vis Spectrophotometer Lamda 35. Data was collected, stored and fitted to zero-, first- and pseudo-second order kinetics model.

3 Results and discussion

3.1 Powder X-ray diffraction

Figure 2 shows the XRD patterns of Zn–Al-LDH and its intercalated compound, Zn–Al-BNOA nanocomposite prepared using various concentrations of BNOA. As shown
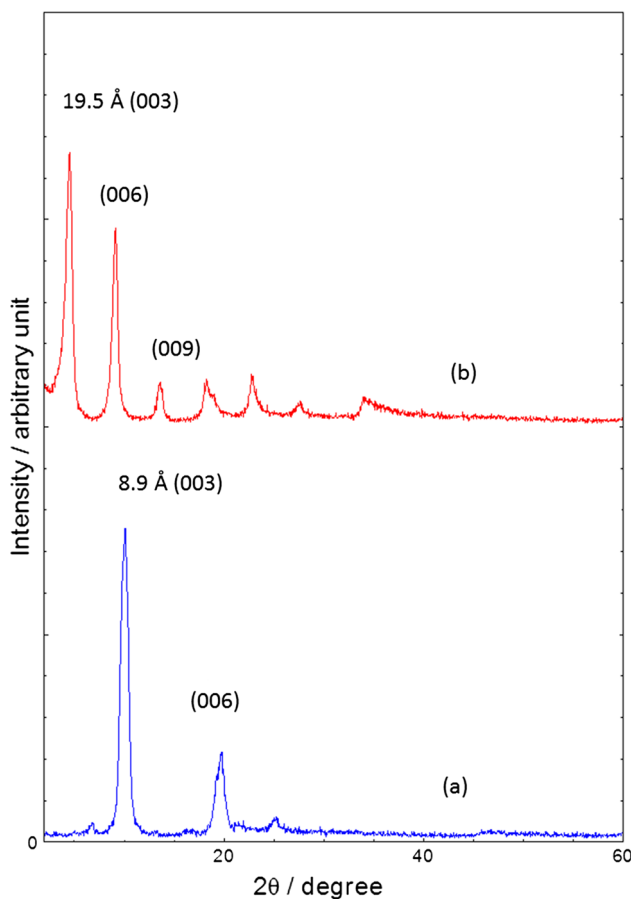

Fig. 2 PXRD patterns for (*a*) Zn–Al-LDH and (*b*) Zn–Al-BNOA

in Fig. 2, the basal spacing for Zn–Al-LDH with nitrate as the interlamella anion is 8.9 Å which is similar to the value reported previously [11]. The XRD pattern for Zn–Al-BNOA nanocomposite is shown in Fig. 2b with basal spacing of 19.5 Å. The expansion of basal spacing from Zn–Al-LDH to Zn–Al-BNOA nanocomposite is due to the inclusion of BNOA into LDH lamellar, and can only be achieved if a suitable concentration of BNOA is available in the mother liquor, under the experimental conditions stated earlier. XRD patterns shown in Fig. 2 are also similar to those previously reported for Zn–Al LDH system [12]. These patterns exhibit some features of layered materials such as narrow, symmetric with high intensity peaks at low 2θ values. The XRD pattern for Zn–Al-BNOA nanocomposite prepared using 0.08 M BNOA, shows sharp, symmetrical and intense peaks especially for (003) peak, indicating a well crystallinity of nanocomposite phase was obtained. Therefore, Zn–Al-BNOA nanocomposite prepared using 0.08 M BNOA was subsequently used for further characterization.

3.2 FTIR spectroscopy

The FTIR spectrum for Zn–Al-LDH shows a broad absorption band at around 3380 cm^{-1} which is due to the presence of OH stretching modes of hydroxyl group of LDH. The band at 1642 cm^{-1} is due to the bending vibration of the interlayer water molecule. A sharp and intense band located at approximately 1345 cm^{-1} is attributed to the stretching vibration of NO_3 [13]. Another band at 679 and 416 cm^{-1} are due to the translation vibrations at Zn-OH and deformation vibration of OH–Zn–Al–OH, respectively [14, 15]. The FTIR spectrum for BNOA (Fig. 3a) shows two bands at 2898 and 2579 cm^{-1} indicated to the OH stretching vibrations. Strong band at 1725 cm^{-1} attributed to the carbonyl, C=O stretching vibration. The bands at 1603 cm^{-1} are due to the stretching vibrations of C=C aromatic rings. The strong band at 1222 cm^{-1} shows the stretching for the C–O–C and the band at 1444 cm^{-1} indicates the presence of CH$_2$ scissoring mode. Strong bands near 744–899 cm^{-1} can be attributed to the presence of phenyl ring substitution [16].

As expected, the FTIR spectrum of Zn–Al-BNOA resembles a mixture of both the spectra of BNOA and Zn–Al-LDH, indicating that both functional groups of BNOA and Zn–Al-LDH are simultaneously present in Zn–Al-BNOA and confirm the intercalation of BNOA in the interlamella of Zn–Al-BNOA. The absorption band at 1345 cm^{-1} which is due to nitrate ions is absent indicates that the anion completely replaced by BNOA anion. This shows that BNOA has higher affinity than nitrate anion towards the inorganic interlamella, thus occupies the interlamella region between the inorganic layers and
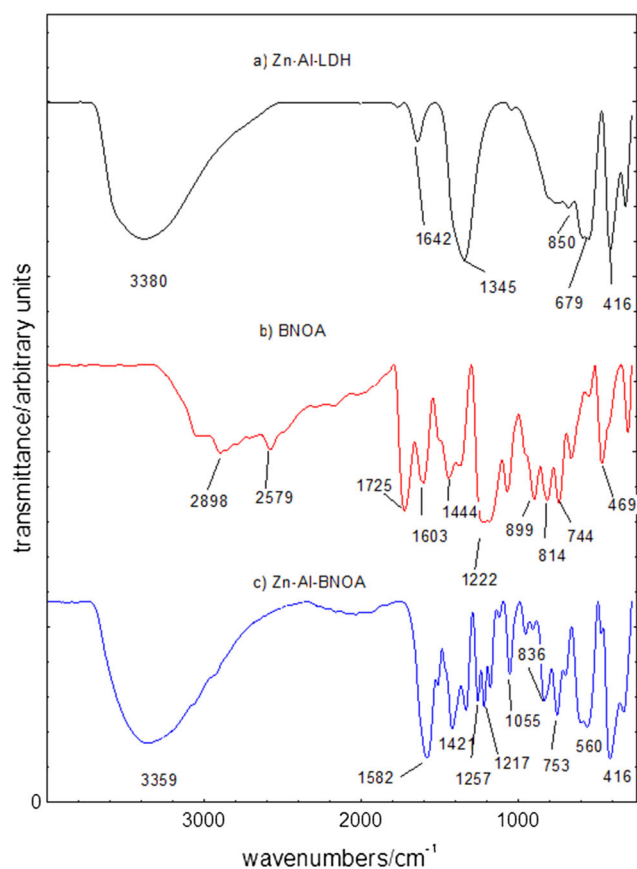
Fig. 3 FTIR spectra for Zn–Al-LDH, BNOA and Zn–Al-BNOA

prevents further co-intercalation of nitrate anion. The most important feature in the FTIR spectra is the disappearance of band 1725 cm^{-1} (due to the carboxylic group) and the presence of new band at around 1582 cm^{-1} which is attributed to C=O carboxylate anion, confirms that the presence of BNOA in the anionic form in the interlayer of the LDH [17].

3.3 Elemental analysis

Table 1 shows the Carbon, Hydrogen, Nitrogen and Sulfur analysis (CHNS) result of Zn–Al-LDH and Zn–Al-BNOA. As shown in the table, Zn–Al-LDH contains 3.0 % nitrogen. This is in agreement with the presence of a strong band at 1345 cm^{-1} in the FTIR spectrum of Zn–Al-LDH shown in Fig. 3, which corresponds to the nitrate group. As expected, CHNS analysis for Zn–Al-BNOA shows no nitrogen, which indicates the absence of this element in Zn–Al-BNOA, as a result of the intercalation of BNOA and the negation of nitrate anion into the interlayer. This is in line with the high content of carbon in Zn–Al-BNOA due to the presence of carbon in BNOA. The percentage of BNOA content in Zn–Al-BNOA is estimated to be 36.2 % (w/w) using CHNS analyzer.

3.4 Isotherm, surface area and pore size distribution

Figure 4 shows the adsorption–desorption isotherm for Zn–Al-LDH and Zn–Al-BNOA nanocomposite material. As shown in the figure, the adsorption–desorption for Zn–Al-BNOA is of type IV, indicating mesoporous-type material (20–500 Å) [18], with adsorption increase rapidly at low relative pressure in the range of 0.05–0.5, followed by a slow uptake of the adsorbent at a higher relative pressure of 0.5–0.8. Further increase of a relative pressure to >0.8 resulted in a rapid adsorption of the adsorbent, reaching an optimum at more than 180 cm^3 g^{-1} at STP. A general shape of the isotherm for Zn–Al-BNOA does not differ very much from Zn–Al-LDH; the type IV isotherm still remains. However, as shown in Fig. 4, the adsorbate uptake is slow in the relative pressure range 0.05–0.9, after which rapid adsorption can be observed. An optimum uptake was about 8 cm^3 g^{-1} at STP, indicates the slow uptake of the nitrogen gas. Desorption branch of the hysteresis loop for Zn–Al-BNOA is much narrower compared to Zn–Al-LDH, indicating different pore texture of the resulting material. This can be related to the different pore structure when nitrate is replaced by BNOA during the formation of Zn–Al-BNOA together with the formation of interstitial pores between the crystallite, and different particle size and morphology.

The surface properties of Zn–Al-LDH and Zn–Al-BNOA are summarized in Table 1. The intercalation of BNOA has increased the BET specific surface area from 1.13 m^2 g^{-1} for Zn–Al-LDH to 42.79 m^2 g^{-1} for Zn–Al-BNOA, which is due to the inclusion of bigger guest anion than the counter anion, nitrate. The intercalation of bigger anion of BNOA resulting in the expansion of basal spacing of the resulting Zn–Al-BNOA nanocomposite and creates more pores in the crystallites, therefore the surface area increased significantly. Table 1 also shows that the BET average pore diameter for Zn–Al-BNOA is lower than that of Zn–Al-LDH, amounting from 203 to 217 Å, respectively. On the other hand, the BJH desorption pore volume of Zn–Al-BNOA is higher than that of Zn–Al-LDH.

The BJH pore size distribution for Zn–Al-LDH and Zn–Al-BNOA are presented in Fig. 5. Both materials show mesoporous type of material, with the adsorption isotherm type IV. BJH pore size distribution for Zn–Al-LDH shows a broad peak at around 200 Å while for Zn–Al-BNOA an intense peak centered at around 300 Å as well as another a very small, weak one at 50 Å. This indicates the modification of pore texture in agreement with the formation of a new intercalated compound, Zn–Al-BNOA with basal spacing of 19.5 Å.

The FESEM micrograph (Fig. 6a, b) illustrates the morphologies of Zn–Al-LDH and Zn–Al-BNOA. Zn–Al-

Table 1 Elemental and Surface properties of Zn–Al-LDH and its intercalated compound, Zn–Al-BNOA

Material	Basal spacing (Å)	% c	% N	BNOA (%w/w)	BET surface area (m² g⁻¹)	BJH desorption pore volume (cm³ g⁻¹)	BET average pore diameter (Å)	BJH average pore diameter (Å)
Zn–Al-LDH	8.93	0.12	3.0	–	1.13	0.010	217	161
Zn–Al-BNOA	19.46	25.6	–	36.2	42.79	0.282	203	199

Fig. 4 Adsorption–desorption isotherms for nitrogen gas at 77 K for Zn–Al-LDH (*a*) and Zn–Al-BNOA (*b*) [also shown in the *inset* with expanded y axis for (*a*)]
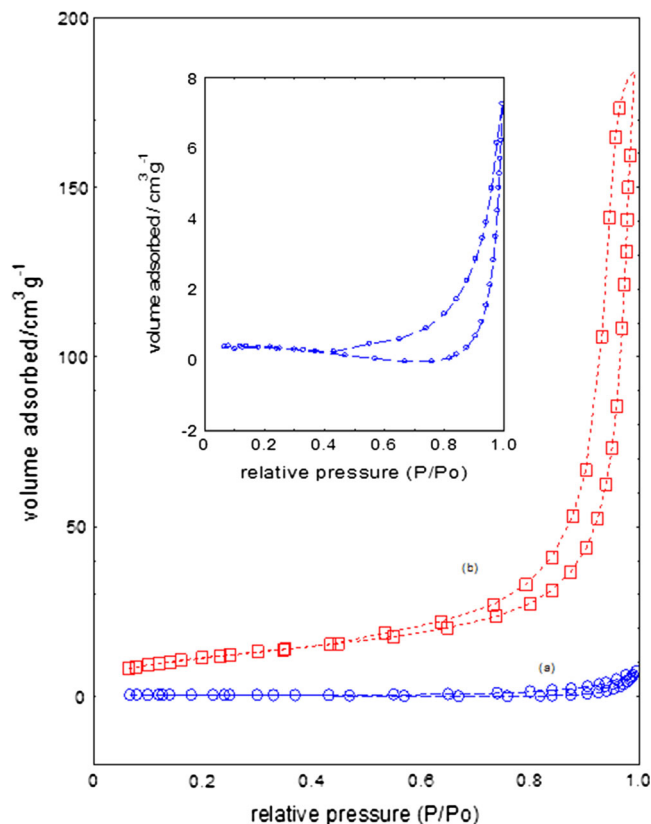
LDH shows a flake-like structure while Zn–Al-BNOA shows a non-uniform irregular agglomerate of compact and non-porous structure. The changes in the morphology of the resulting material are due to the inclusion of BNOA into the interlayer spaces of Zn–Al layered double hydroxide.

3.5 Release of BNOA into aqueous solution

Figure 7 shows the release profile of BNOA from the interlamella of Zn–Al-BNOA into 0.005 M sodium phosphate (Na_3PO_4), sodium carbonate (Na_2CO_3), sodium sulfate (Na_2SO_4) and sodium chloride (NaCl) solutions. The release rate was found to be faster in the first 300 min followed by slower released until the equilibrium achieved at around 900 min. The amount of BNOA released from Zn–Al-BNOA into aqueous solution containing Na_3PO_4 was found to be the highest. It was observed that at the end of rapid release rate, the amount of BNOA released from Na_3PO_4 aqueous solution was 86 % followed by 79 and 40 % for Na_2CO_3 and Na_2SO_4, respectively. The lowest percentage of BNOA released was achieved in NaCl aqueous solution. At equilibrium, it was estimated that only about 15 % of BNOA could be released from Zn–Al-BNOA into the aqueous solution. Therefore, the order of BNOA released from Zn–Al-BNOA at the end 1500 min can be summarized as $Na_3PO_4 > Na_2CO_3 > Na_2SO_4 > NaCl$ [19].

The amount of BNOA released at equilibrium is higher for Na_3PO_4 solutions followed by Na_2CO_3, Na_2SO_4 and NaCl. In general, several factor such as the affinity of the anion towards the Zn–Al-LDH inorganic interlamellae is important and will contribute to the amount of BNOA released into the aqueous solution. The selectivity for the

Fig. 5 BJH pore size distribution for (*a*) Zn–Al-LDH and (*b*) Zn–Al-BNOA [also shown in the *inset* with expanded y axis for (*a*)]
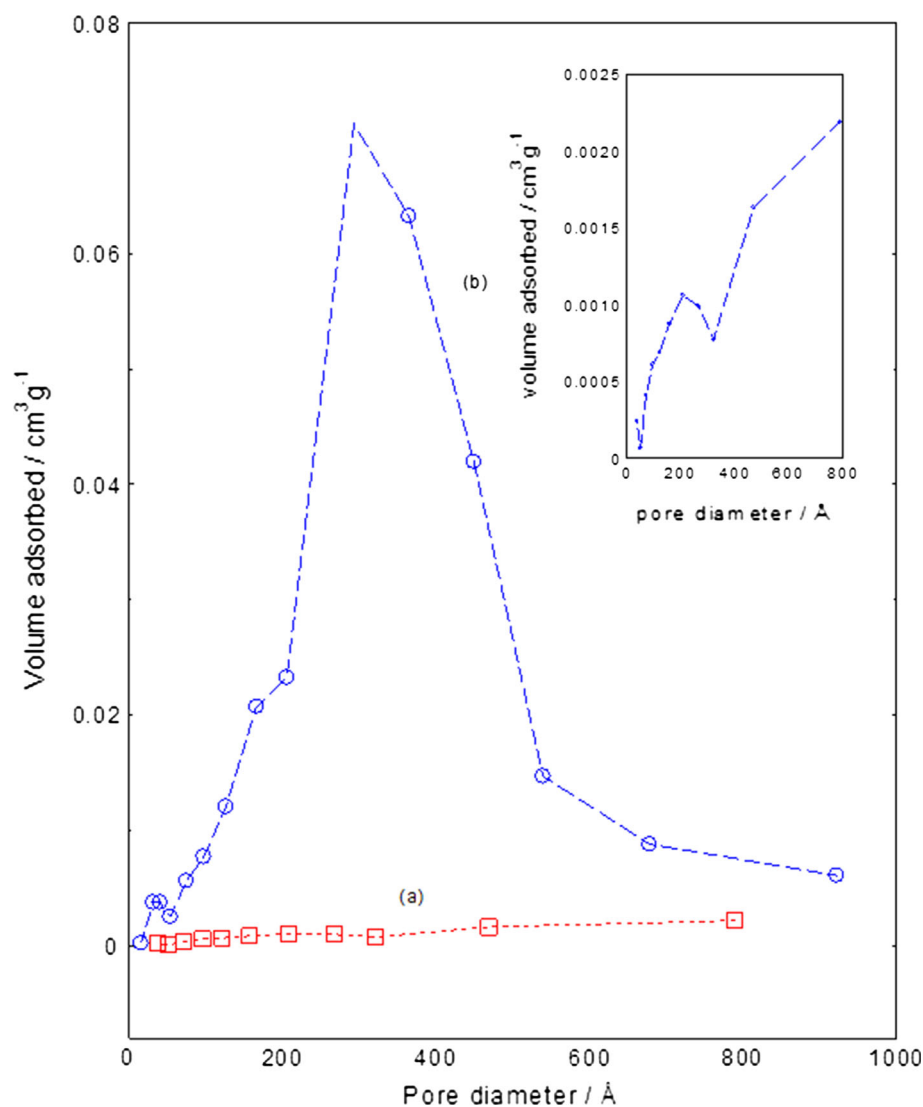
Zn–Al-LDH increases with the increasing electric charge of the anion and the decreasing anion size, for example $PO_4^{3-} > CO_3^{2-} > SO_4^{2-} > OH^- > F^- > Cl^- > Br^- > NO_3^- > I^-$ [19]. The anion, which has highest electric density, exhibits the highest electrostatic force toward the host layer. Trivalent anion such as PO_4^{3-} and divalent anions like CO_3^{2-} and SO_4^{2-} have higher selectivity than monovalent anions.

The rapid release pattern of the anions is obvious if only ion exchange phenomenon governs the release of BNOA into the aqueous media. At the beginning of the experiment, the ion exchanged of BNOA with a smaller anion, resulted in a decrease in the basal spacing and this phase transformation will first cover the external part of the nanohybrid crystals. As the reaction proceeded, a smaller and a larger basal spacing co-existed in the same crystal and therefore a formation of phase boundary between internal zones containing LDH occurred. As a result of the

formation of this new phase (LDH), a sort of 'barrier' builds up between controlled release formulation, Zn–Al-BNOA and the aqueous solution, and consequently this will further decrease the rate of the BNOA that could be released from the formulation into the aqueous solution, hence the amount of BNOA released declined progressively [20].

3.5.1 Kinetic release

In order to get some insight into the kinetics release of the BNOA anions from the nanohybrids, quantitative analysis of the data obtained from the release study were fitted to zeroth order, first order and pseudo-second order. It was suggested that the herbicide release based on herbicide-LDHs system could be controlled either by dissolution of LDH or by diffusion through the LDH [21]. A single straight line was employed to fit the experimental data as
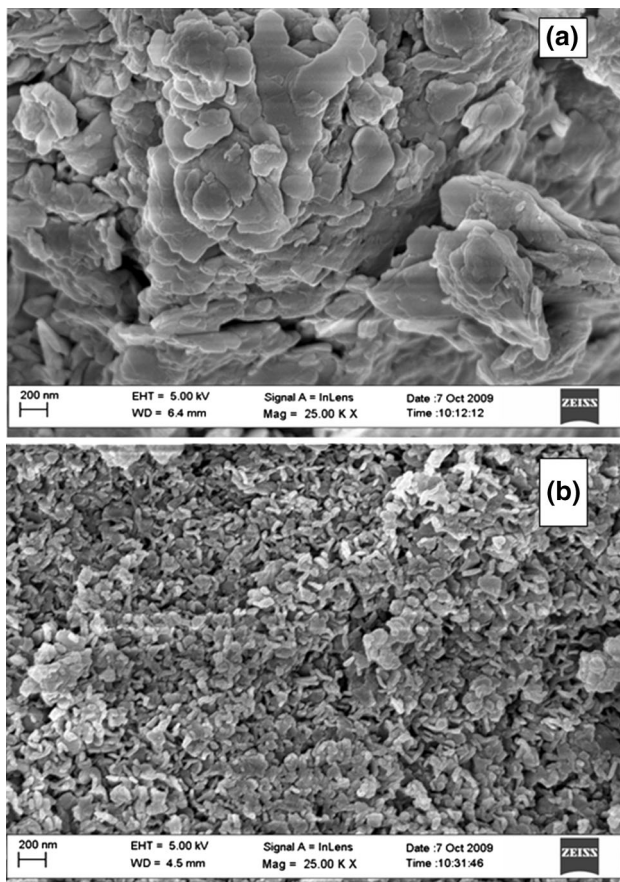
Fig. 6 Scanning electron micrograph for **a** Zn–Al-LDH and **b** Zn–Al-BNOA at 25,000×

Fig. 7 Release profile of BNOA ion into 0.005 M (*a*) Na₃PO₄, (*b*) Na₂CO₃, (*c*) Na₂SO₄ and (*d*) NaCl aqueous solution

described in the previous literature [21], where the release kinetics was studied for intercalated clay minerals. The following zeroth [Eq. (1)] [22], first-order [Eq. (2)] [23] and pseudo-second order [Eq. (3)] [24], equations are given below in which C_{eq} and C_t is the percentage release of the herbicides at equilibrium and time, t, respectively, and c is a constant.

$$C_t = kt + c \tag{1}$$

$$-\log(1 - C_t) = kt + c \tag{2}$$

$$t/C_t = 1/k_2 C_{eq}^2 + (1/q_e) \cdot t \tag{3}$$

The release profiles fitted to zeroth, first and pseudo-second order equations are given in Fig. 8. The extent of time in which the values are fitted to the equation and the regression are given in Table 2. As shown in Fig. 8 and in Table 2, the release of BNOA into 0.005 M NaCl, Na₂CO₃, Na₃PO₄ and Na₂SO₄ of aqueous solutions was found to be nicely fitted to the zeroth and first order equation for the first 200 min with regression values of around 0.900. Poor fitting to the fitting of data for the pseudo-second order kinetics for the short-time range. However, the release profiles follow nicely to the pseudo-second order
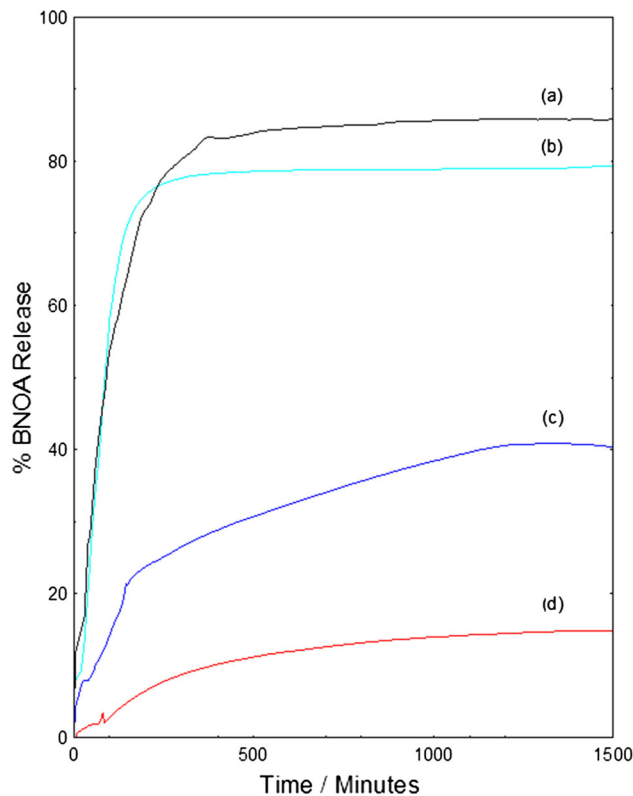
kinetics for the long-time range of the ion-exchange process up to 1500 min with regression values around 1.000. The release of BNOA from the inorganic LDH interlamellae involved dissolution of the nanocomposite as well as ion-exchange between the intercalated anions in the interlamellae host and the chloride, sulfate, carbonate and phosphate anions in the aqueous solution can be better describe by zeroth and first order at the beginning of the release process from 0 until 200 min but for the whole process it is controlled by pseudo second order kinetic model as reflected by the regression, r^2 values.

3.5.2 PXRD study on the reclaimed samples in 0.005 M Na₂CO₃

In order to understand the ion exchange process and the related phenomena, the resulting samples were recovered from the aqueous solution after the released experiment. Zn–Al-BNOA selected from various contact times were reclaimed, thoroughly washed, dried and characterized by PXRD. The PXRD patterns for the recovered samples are shown in Fig. 9. The PXRD of LDH-CO₃ with carbonate as the counter anion, were also shown in Fig. 9a for comparison. As shown in Fig. 9, the 003 reflection for BNOA nanohybrids phase reduced in intensity after it was
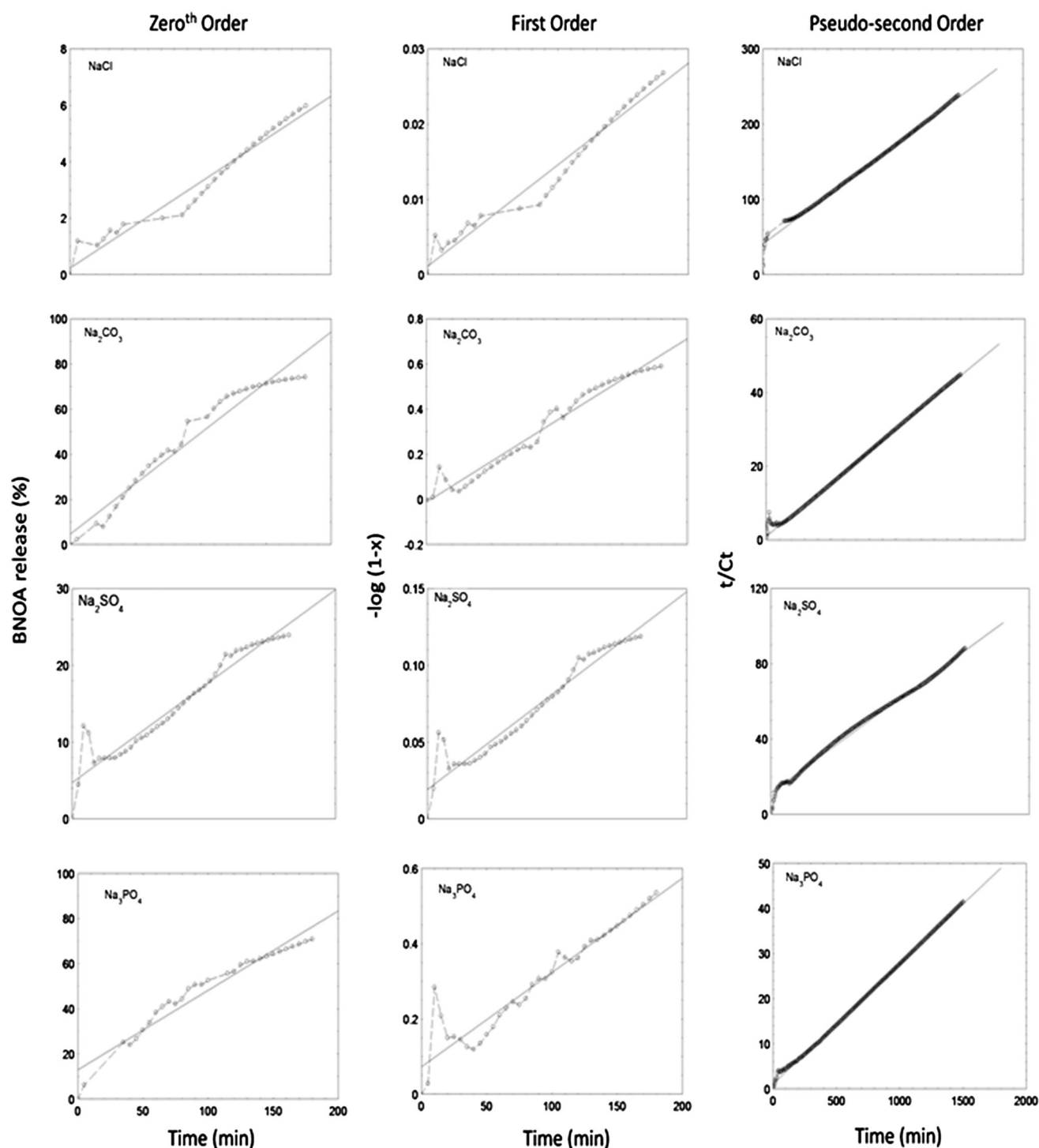
Fig. 8 Fitting the release data of BNOA anion from Zn–Al-BNOA into various media using zeroth, first and pseudo second order kinetic models for release time 0–200 min and 0–1500 min

contacted with the aqueous solutions for 10 min to 24 h contact time.

The 'new' LDH phase, which was believed to be Zn–Al-LDH with carbonate as the counter anion was formed as a result of the anion-exchange process between the outgoing

anion (BNOA) intercalated into the nanohybrids with the incoming anion from Na₂CO₃ solution. These 'new' LDH phases can be clearly observed and the formation of this phase increased as the contact time increased (Fig. 9). The PXRD result shows that this is the case in which the basal
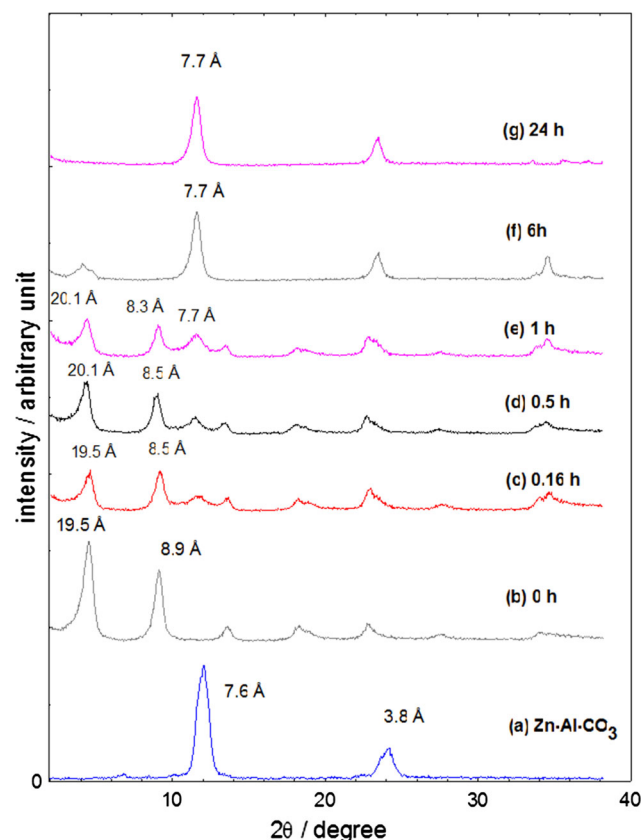
Table 2 Fitting the release data of BNOA anion from Zn–Al-BNOA into various media using zeroth, first and pseudo second order kinetic models for release time 0–200 min and 0–1500 min

Aqueous solution 0.005 M	Release time (min)	Zeroth order r^2	First order r^2	Pseudo second order, r^2
NaCl	200	0.960	0.963	0.667
	1500	0.796	0.810	0.995
Na_2SO_4	200	0.932	0.938	0.735
	1500	0.825	0.873	0.993
Na_2CO_3	200	0.955	0.966	0.172
	1500	0.233	0.325	0.997
Na_3PO_4	200	0.943	0.909	0.852
	1500	0.367	0.563	0.999

spacing of the as-synthesized LDH with carbonate as the counter anion synthesized in this work show similar characteristics.

This study shows the sequence of events involved on the release of BNOA into the aqueous solution has resulted in the decomposition of the nanohybrid phase and the collapsed of the layered structure followed by the formation of LDH. The release of BNOA anion from the interlayer Zn–Al-BNOA into the aqueous solution containing sodium

Fig. 9 PXRD patterns for Zn–Al-BNOA samples reclaimed from 0.005 M Na_2CO_3 aqueous solution at various release times, 0–24 h

carbonate could have occurred in at least two ways. The conservation of the layered nanohybrid phase after 1 h released time showed that the release of BNOA anion from the interlayer of Zn–Al-BNOA probably occurred via ion exchange mechanism, in which the BNOA anions were exchanged with CO_3^{2-} ions and were released into the aqueous solution and the PXRD patterns of the recovered samples after 24 h showed that the layered structure fully collapsed. This showed that almost all the BNOA anions in the interlayer of Zn–Al-BNOA were released into the aqueous solution resulting in the collapse of Zn–Al-BNOA structure. At the same time, LDH containing carbonate as the counter anion formed as observed in the PXRD pattern with basal spacing of 7.7 Å [25].

4 Conclusion

A new Zn–Al-BNOA nanohybrid material was successfully synthesized with BNOA, as the active agent inserted into the interlayer structure of Zn–Al layered double hydroxide. The expansion of basal spacing of Zn–Al-LDH from 8.9 to 19.5 Å indicates that the successfully of BNOA intercalation into intergallery of LDH. This is confirmed and supported by FTIR and CHNS results, which shows the presence of COO^- of BNOA group in Zn–Al-BNOA material. The BET surface area increased from 1.13 to 42.79 $m^2\ g^{-1}$ for Zn–Al-LDH and its intercalated compound, Zn–Al-BNOA, respectively if 0.08 M BNOA was used for the synthesis of the latter. The release of the BNOA anion from the interlamellae of Zn–Al-BNOA nanocomposite was controlled by the zeroth and first order kinetics at the beginning of the deintercalation process up to 200 min and controlled by pseudo-second order kinetics for the whole process. This study suggests that layered double hydroxide can be used as a carrier for an active agent and the chemical structure of the intercalated moiety

can be used to tune the desired release duration of the beneficial agent.

References

1. M.M. Shaijumon, N. Bejoy, S. Ramaprabu, Appl. Surf. Sci. **242**, 192 (2005)
2. A.H. Yahaya, M.Z. Hussein, W.S. She, J. Phys. Chem. Solids **3**, 64 (2006)
3. M.Z. Hussein, Z. Zainal, T.C. Beng, J. Environ. Sci. Health. Part A Toxic/Hazard. Subst. Environ. Eng. **36**, 565 (2001)
4. P. Gunawan, R. Xu, J. Pharm. Sci. **97**, 4367 (2008)
5. M.Z. Hussein, Z.B. Jubri, Z. Zainal, A.H. Yahya, Mater. Sci. Pol. **22**, 57 (2004)
6. M.Z. Hussein, C.W. Long, Mater. Chem. Phys. **85**, 427 (2004)
7. P.S. Braterman, Z.P. Xu, F. Yarberry, in *Handbook of Layered Materials*, ed. by S.M. Auerbach, K.A. Carrado, P.K. Dutta (Marcel Dekker, Inc., New York, 2004), pp. 373–474
8. M.Z. Hussein, T.K. Hwa, J. Nanoparticle Res. **2**, 293 (2000)
9. S.H. Sarijo, A. Ahmad, Z. Jubri, Adv. Mater. Res. **422**, 102 (2012)
10. J.L. Muller, Plant Growth Regul. **32**, 219 (2000)
11. M.M. Md Najat, K. Yusoff, M.Z. Hussein, Curr. Nanosci. **4**, 391 (2008)
12. M.Z. Hussein, M.Y. Ghotbi, A.H. Yahaya, M.Z.A. Rahman, Mater. Chem. Phys. **113**, 491 (2009)
13. Z. Jubri, M.Z. Hussein, A. Yahaya, Z. Zainal, Nanosci. Methods **1**, 152 (2012)
14. M.Z. Hussein, Z. Zainal, A.H. Yahaya, S.H. Sarijo, in *Proceedings of Conference on Advanced Materials 2005 (CAM 2005)*, (2005), p. 302
15. M. Lakraimi, A. Legrouri, A. Barroug, A.D. Roy, J.P. Besse, J. Mater. Chem. **10**, 1007 (2000)
16. R.M. Silverstein, T.C. Morill, G.C. Bassler, *Spectrometric Identification of Organic compounds* (Wiley, New York, 1998), pp. 110–125
17. M.Z. Hussein, S.H. Sarijo, A.H. Yahaya, Z. Zainal, Nanosci. Nanotechnol. **7**, 1 (2007)
18. K.S.W. Sing, D.H. Everett, R.A.W. Haul, L. Moscou, R.A. Pierotti, J. Rouquerol, T. Siemieniewska, Pure Appl. Chem. **57**, 603 (1985)
19. A. Tsujimura, M. Uchida, A. Okuwaki, J. Hazard. Mater. **143**, 582 (2007)
20. M.Z. Hussein, A.H. Yahaya, Z. Zainal, L.H. Kian, Sci. Technol. Adv. Mater. **6**, 956 (2005)
21. H. Jung, H.M. Kim, Y.B. Choy, S.J. Hwang, J.H. Choy, Int. J. Pharm. **349**, 283 (2008)
22. S. Miyata, Clays Clay Min. **28**, 50 (1980)
23. S.P. Newman, W. Jones, N. J. Chem **22**, 105 (1998)
24. M. Vucelic, W. Jones, G.D. Moggridge, Clays Clay Min. **6**, 803 (1997)
25. O.C. Wilson, T. Olorunyolemi, A. Jaworski, L. Borum, D. Young, A. Siriwat, C. Oriaki, M. Lerner, Appl. Clay Sci. **15**, 265 (1999)